Immune factor of bacterial origin protects ticks against host microbial commensals

Authors: Beth M. Hayes[1*], Atanas D. Radkov[1*], Fauna Yarza[1], Sebastian Flores[1], Jungyun Kim[1], Ziyi Zhao[1], Katrina W Lexa[2], Liron Marnin[3], Jacob Biboy[4], Victoria Bowcut[1], Waldemar Vollmer[4], Joao HF Pedra[3], Seemay Chou[1,5†].

Affiliations:

[1]Department of Biochemistry and Biophysics, University of California, San Francisco, San Francisco, CA 94158, USA.

[2]Modeling and Informatics, MRL, Merck Sharp & Dohme, Rahway, New Jersey 07065, USA.

[3] Department of Microbiology and Immunology, University of Maryland School of Medicine, Baltimore, MD, USA.

[4] Centre for Bacterial Cell Biology, Biosciences Institute, Newcastle University, Newcastle upon Tyne, UK.

[5]Chan Zuckerberg Biohub, San Francisco, CA 94158, USA.

*These authors contributed equally.

[†]Correspondence to: seemay.chou@ucsf.edu

Abstract:

Hard ticks interface with diverse microbes while feeding on vertebrate hosts. We previously discovered that ticks horizontally acquired an antimicrobial toxin gene from bacteria known as *domesticated amidase effector 2* (*dae2)*. Here we show that this effector from the tick disease vector *Ixodes scapularis* (Dae2^{Is}) is delivered to the host bite site via saliva and that its structural and biochemical divergence from bacterial homologs results in an expanded targeting range to include host skin microbes. Upon disruption of *dae2*^{Is}, we found higher loads of skin-associated staphylococci within ticks, adversely affecting their fitness. In contrast, Dae2^{Is} has no intrinsic lytic activity against *Borrelia burgdorferi,* the tick-borne pathogen of Lyme disease. Our observations suggest ticks have evolved to preferentially resist opportunistic pathogens, such as host skin commensals, while tolerating their own symbionts. These results highlight a unique interkingdom interface between blood-feeding vectors, hosts, and their associated microbes where incompatible host-microbe interactions lead to disease.

Main text:

Blood-feeding (hematophagy) arose independently in at least six different arthropod lineages approximately 50-150 MYA, coincident with the emergence of a wide array of key host-modulating genes that support this specialized lifestyle[1-3]. The blacklegged tick *Ixodes scapularis* requires an exceptionally prolonged, continuous bloodmeal in order to transition between each of its three life stages[4]. Ticks must establish an intimate attachment into the dermis of a bloodmeal host during this period for up to a week in length. To maintain this perilous yet essential interaction, ticks encode a cocktail of salivary molecules deployed at the bite site to block host immune and sensory responses while promoting blood flow[5-7]. Adapting to bloodmeal hosts also necessitates contending with host-associated microbes that can infect the tick or the tick bite site. Thus, the nature and selectivity of tick salivary activities provide a unique window into the evolutionary history of complex multi-kingdom interactions between ticks, their hosts, and microbes[6,8].

I. scapularis ticks employ a diverse repertoire of immune effectors, including antimicrobial peptides and lysozyme-like enzymes[9-11]. We previously found that *I. scapularis* and other ticks acquired a potent antibacterial enzyme approximately 40 MYA by domesticating an interbacterial competition toxin gene from bacteria[12]. The horizontally co-opted bacterial type VI secretion (T6S) amidase effector 2 (*tae2*) gene family encodes lytic cell wall-degrading enzymes delivered to rival Gram-negative bacteria by specialized bacterial T6SS machinery [13,14]. Tae2 toxins encode hydrolases that break down the Gram-negative bacterial cell wall peptidoglycan (PG) of recipient microbes, resulting in osmotic stress and subsequent cell lysis. In contrast, the representative in ticks, domesticated amidase effector 2 (Dae2), does not have a specialized delivery system that allows it to cross the outer membrane of Gram-negative bacteria to access the PG and thus is not intrinsically capable of gaining physical access to cell walls of Gram-negative bacteria due to their protective outer membrane[12]. Thus, it remains unknown whether Dae2 has been acquired by ticks to directly lyse bacteria. However, given the rarity of interkingdom gene transfer and subsequent gene conservation[15], *dae2* likely confers an important adaptive advantage to ticks. Understanding the biological function of Dae2 could provide clues as to which microbes pose a threat to their blood-feeding lifestyle.

The microbiota of ticks are dominated by a few bacterial symbionts that are also transmissible human pathogens, including *Rickettsia spp.* and *Borrelia burgdorferi*, the causative agent of Lyme disease[16-21]. Our prior work revealed that *dae2*^{Is} modestly limits *B. burgdorferi* proliferation in *I. scapularis*[12]. Dae2 may prevent excessive *B. burgdorferi* proliferation that may be detrimental to ticks. Alternatively, Dae2^{Is} may primarily act on other bacteria in unknown ways, such as protecting against natural tick pathogens that have not been previously characterized. Here we report that the structural and biochemical divergence of *I. scapularis*-encoded Dae2^{Is} from its ancestral bacterial counterparts results in a broadened antibacterial specificity, which extends its efficacy to Gram-positive bacteria that are enriched in the skin microbiota of mammals. Through its action in both the tick gut and saliva during feeding, Dae2^{Is} directly antagonizes bacterial commensals of bloodmeal host skin, which are detrimental to both the viability and feeding success of ticks.

Structural analysis of Tae2 and Dae2 enzymes

Evolutionary divergence of a gene following horizontal acquisition is driven by the biology of its recipient organism. A sequence-based alignment of the domesticated *dae2* genes from ticks and mites with ancestral bacterial *tae2* homologs showed several regions of variance between these groupings (Figure S1a-b). Although we were unable to definitively find evidence of positive or negative selection[12], these variances were unique to eukaryotic representatives and highly suggestive of functional differences, such as substrate specificity. To investigate this possibility, we determined the high-resolution structure of Tae2 from *Salmonella enterica* Typhi ($Tae2^{St}$) at a resolution of 2.05 Å by X-ray crystallography (Figure 1a, Table 1, PDB ID: 6W1N).

$Tae2^{St}$ adopts a canonical papain-like amidase fold with a closest structural homolog of endolysin LysK from staphylococcal phage K (Figure S2)[22]. Guided by a structure-based alignment, we compared threaded $Tae2^{St}$ and $Dae2^{Is}$ structures, which pointed to several key differences between eukaryotic and prokaryotic subgroups. Three major regions of sequence divergence mapped to the loops (L1-L3) that abut the catalytic channel (Figure 1b), which could affect the selectivity of interactions between these enzymes and their bacterial cell wall PG substrates. This comparison also revealed substantial differences in the topology and electrostatic properties of a deep hydrophobic substrate-binding groove that extends from the active site (Figure 1c-d). The catalytic residues themselves are more accessible in $Dae2^{Is}$ than in $Tae2^{St}$, with a predicted pore behind the catalytic cysteine of $Dae2^{Is}$, which could provide substantial contact area for interactions with branched PG chains. Surface conservation profiles (Figure S3) further suggested that these divergent properties are conserved within Tae2 and Dae2 subgroups, respectively. Overall, the catalytic channel for Dae2 appears to be distinct and splayed more open relative to that of Tae2, suggesting substrate specificity of the eukaryotic enzymes could either be distinct or expanded from the bacterial enzymes.

Comparison of Tae2 and Dae2 cell wall specificities

The specificity of Dae2 for bacterial cell wall PG would dictate which microbes can be inhibited through Dae2, which we first examined *in silico*. Notably, PG chemical composition varies considerably between bacterial taxa, particularly at the third residue position within the peptide stem (Figure 2a)[23]; thus the amino acid at that position could influence or determine Dae2 specificity. For instance, Gram-negative bacteria incorporate *meso*-diaminopimelic acid (*m*DAP) at this variable third position, whereas bacteria from the class Bacillus have an amidated *m*DAP and other Gram-positive species have a lysine[23]. We previously found that both Tae2 and Dae2 can hydrolyze Gram-negative cell walls[12]. To compare substrate interaction surfaces, we computationally docked a fragment of crosslinked *m*DAP PG onto $Tae2^{St}$ and $Dae2^{Is}$ (Figure 2b-e). Docked PG adopted highly dissimilar poses between the two structures. We calculated an overall narrower cleft on $Tae2^{St}$ with 852.9 $Å^2$ active site surface area versus 1086.0 $Å^2$ for $Dae2^{Is}$, which also has an additional deep binding pocket. Upon binding, the cross-linked PG buried the binding surface significantly more in $Dae2^{Is}$ than $Tae2^{St}$, with a delta of 624.9 $Å^2$ compared to 450.2 $Å^2$. Our modeling and metadynamics simulations predicted a flipped PG orientation mediated through different residue interactions at the enzyme–substrate binding interface (Figure S3c-d) as well as tighter substrate binding. Using this information, our modeling predicted a flipped PG orientation mediated through different residue interactions at the enzyme–substrate binding interface (Figure S3c-d). Altered positioning of the PG substrate

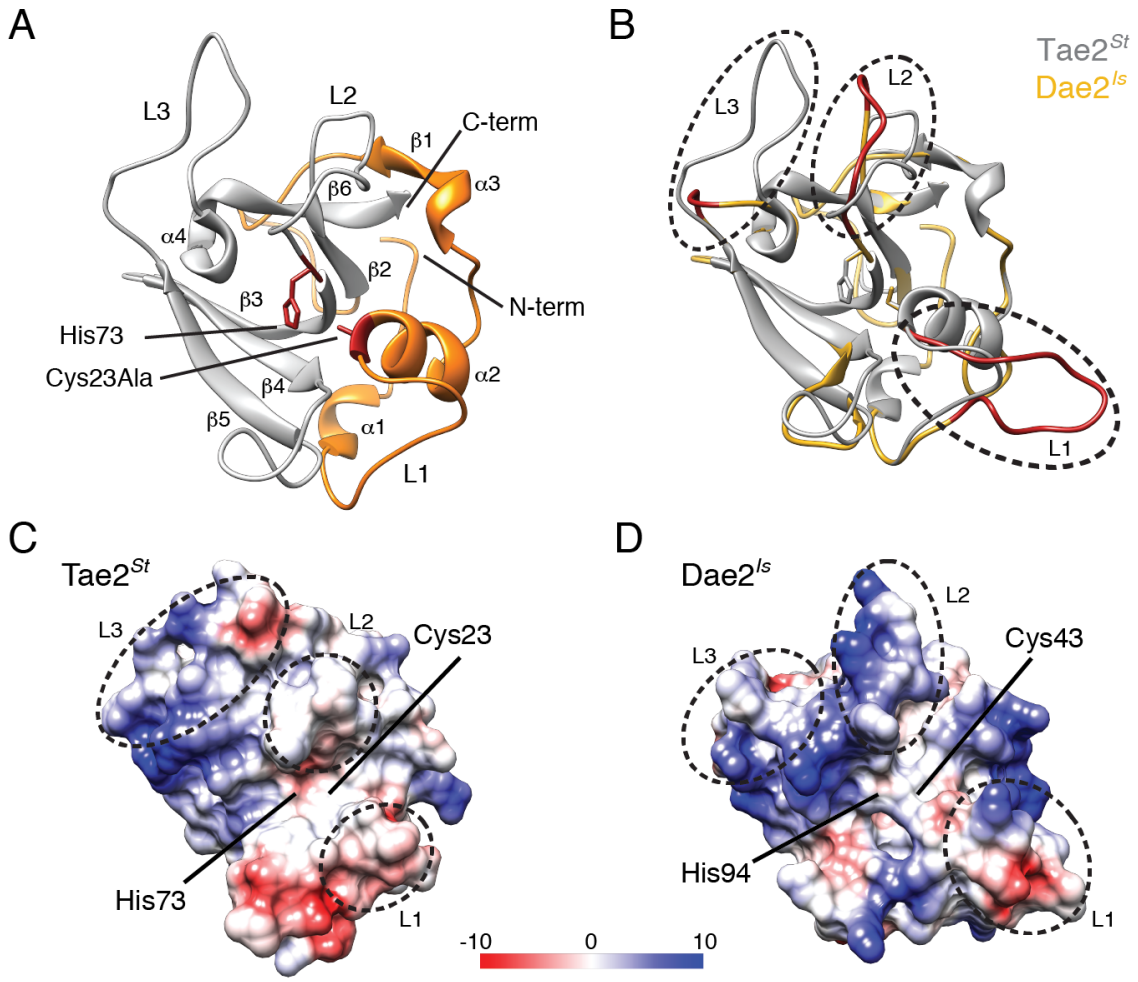

Figure 1: Comparison of Tae2 and Dae2 structures. (**A**) Ribbon diagram Tae2 from *Salmonella enterica* Typhi (Tae2St). Canonical papain-like secondary structures are labeled (α1-4, β1-6, Loop1-3 (L1-3)), and subdomains are colored (gray, orange). Catalytic residues are denoted (labeled His 73 and Cys23Ala, red). (**B**) Structural alignment of Tae2St (gray) and a Tae2-based model of Dae2^{Is} (golden). Loops 1, 2, and 3 are colored red in Dae2^{Is}. (**C, D**) Electrostatic charges in surfaces proximal to the catalytic residues for Tae2St (C) and Dae2^{Is} (D) (Scale is in kcal mol^{-1} e^{-1}). The loops are also boxed in the alignment (**Fig. S1**).

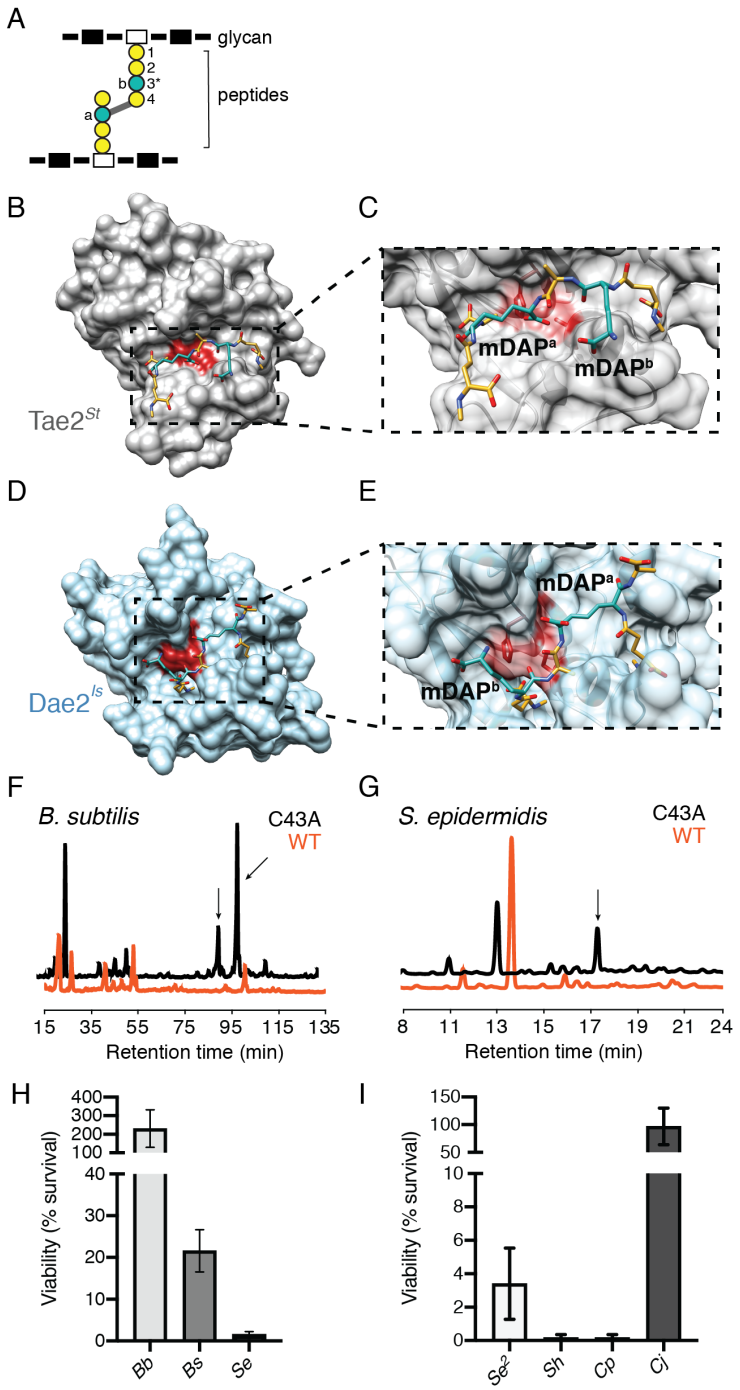

Figure 2: Enzymatic and antibacterial specificity of Tae2 and Dae2. (**A**) Cartoon schematic of bacterial peptidoglycan (PG) structure with glycans (rectangles), peptides (circles), and cross-link position (gray line) shown. Residue positions in PG peptide stem are labeled (1-4) with key variable third position (3*) colored in teal. (**B**) Surface representation of Tae2St ligand docking using a stem peptide substrate. Both *m*DAP residues in the stem peptide are colored in teal. (**C**) Close-up of the Tae2St active site and docked substrate. The scissile amide bond is between *m*DAP^{a} and the adjacent D-ala (position 4), proximal to the active site Cys23 residue. (**D**) Surface representation of Dae2^{Is} ligand docking, using the same substrate as for Tae2St in C. (**E**) Close-up of the Dae2^{Is} active site and docked substrate. The scissile bond is similarly situated between *m*DAP^{a} and the adjacent D-ala, proximal to the active site Cys43 residue. Notice the substrate directionality being *m*DAP^{b} – D-ala – *m*DAP^{a}, compared to the inverse for Tae2St, *m*DAP^{a} – D-ala – *m*DAP^{b}. HPLC chromatograms of PG from *B. subtilis* (**F**) and *S. epidermidis* (**G**) after enzymatic degradation with Dae2^{Is} wt (orange) and its catalytically inactive mutant (C43A, black). Arrows indicate the substrate peaks. Dae2^{Is} lysis assays of (**H**) Gram-negative *Borrelia burgdorferi* strain S9 (*Bb*), Gram-positive *Bacillus subtilis* 168 (*Bs*), and Gram-positive *Staphylococcus epidermidis* BCM060 (Se) and (**I**) Gram-positive skin associated bacteria *S. epidermidis* strain SK135 (*Se*^{2}), *S. hominis* strain SK119 (*Sh*), *Corynebacterium propinquum* DSM44285 (*Cp*) and *C. jeikeium* DSM7171 (*Cj*). Results are reported as percent survival with Dae2^{Is} wt normalized to its catalytic mutant Dae2^{Is} C43A.

could affect recognition or binding of different cell wall types, which we hypothesize leads to a unique and potentially more promiscuous bacterial targeting range for Dae2 enzymes. In summary, our *in silico* modeling predicts that Dae2 enzymes can act on different PG structural groups than the bacterial Tae2 enzymes, modifying or widening the range of antagonized bacteria *in vivo*.

We therefore comprehensively examined the *in vitro* substrate specificity of Dae2^{Is} and Tae2St. To define biochemical specificity, we tested enzymes against a set of PG sacculi prepared from bacteria that we and others have found associated with field *I. scapularis* ticks: two environmental species (*Escherichia coli, Bacillus subtilis*) and a mammalian skin-associated bacterium (*Staphylococcus epidermidis*)[18,24]. Analysis of PG degradation by high performance liquid chromatography (HPLC) showed that the bacterial Tae2St-dependent hydrolysis is restricted to Gram-negative cell walls (Figure S4a-c), consistent with the restricted role Tae2 toxins play in contact-dependent T6S interbacterial competition specifically between Gram-negative bacteria. In contrast, Dae2^{Is} hydrolyzed all PG sacculi types tested (Figure 2f-g). Expansion of Dae2^{Is} specificity to encompass Gram-positive *S. epidermidis* was particularly remarkable, given how divergent its cell wall composition is from that of Gram-negative bacteria. These biochemical analyses imply that Dae2^{Is} has evolved to antagonize a wider range of microbes.

Selectivity of Dae2^{Is} antimicrobial activity

We tested whether our *in vitro* substrate hydrolysis data indeed reflect broadened antibacterial activity by quantifying Dae2^{Is} effects on the viability of bacterial cells. We carried out bacterial toxicity assays at a physiologically relevant concentration of 2 μM Dae2^{Is}, which was estimated by Western blot analysis of dissected *I. scapularis* salivary glands (Figure S5). *E. coli* is intrinsically resistant to Dae2^{Is} as it is not able to penetrate the outer membrane surface of *E. coli* to degrade PG[12]. This is also true for the tick-borne spirochete *B. burgdorferi* (Figure 2h), which has an unusual outer membrane structure that is highly distinct from *E. coli*[25,26]. Thus, the role of Dae2^{Is} against Gram-negative species is likely restricted to immunoregulatory processing of PG fragments or requires collaboration with another co-factor. In stark contrast, Dae2^{Is} promotes highly efficient killing of a human skin commensal *S. epidermidis* strain and moderate killing of *B. subtilis* (Figure 2h). This observation led us to hypothesize that skin microbes, which are frequently encountered by feeding ticks, are important antibacterial targets for *I. scapularis*. We further tested Dae2^{Is} against three additional skin commensal species: another *S. epidermidis* strain, *S. hominis* and *Corynebacterium propiquum,* and observed immediate lysis of all (Figure 2i). Although related to *C. propiquum* and associated with human skin and mucus membranes, we did not see killing of *C. jeikeium* by Dae2^{Is}, suggesting that Dae2 specificity is broad but not indiscriminate. It is possible that this more invasive strain of *Corynebacterium* has evolved mechanisms of resistance to cell wall targeting enzymes[27]. Together, our analyses led to two major conclusions. First, expansion of Dae2 enzyme specificity potentiates inhibition of a broader set of microbes. Second, the most efficiently targeted bacteria we tested were common skin commensals, which reside at the tick–host interface.

Localization of Dae2^{Is} during requisite bloodmeals

While feeding, ticks secrete a cadre of salivary molecules to maintain bite site sterility and modulate host processes, such as immune and sensory responses (Figure 3a) [3,28]. Thus, we

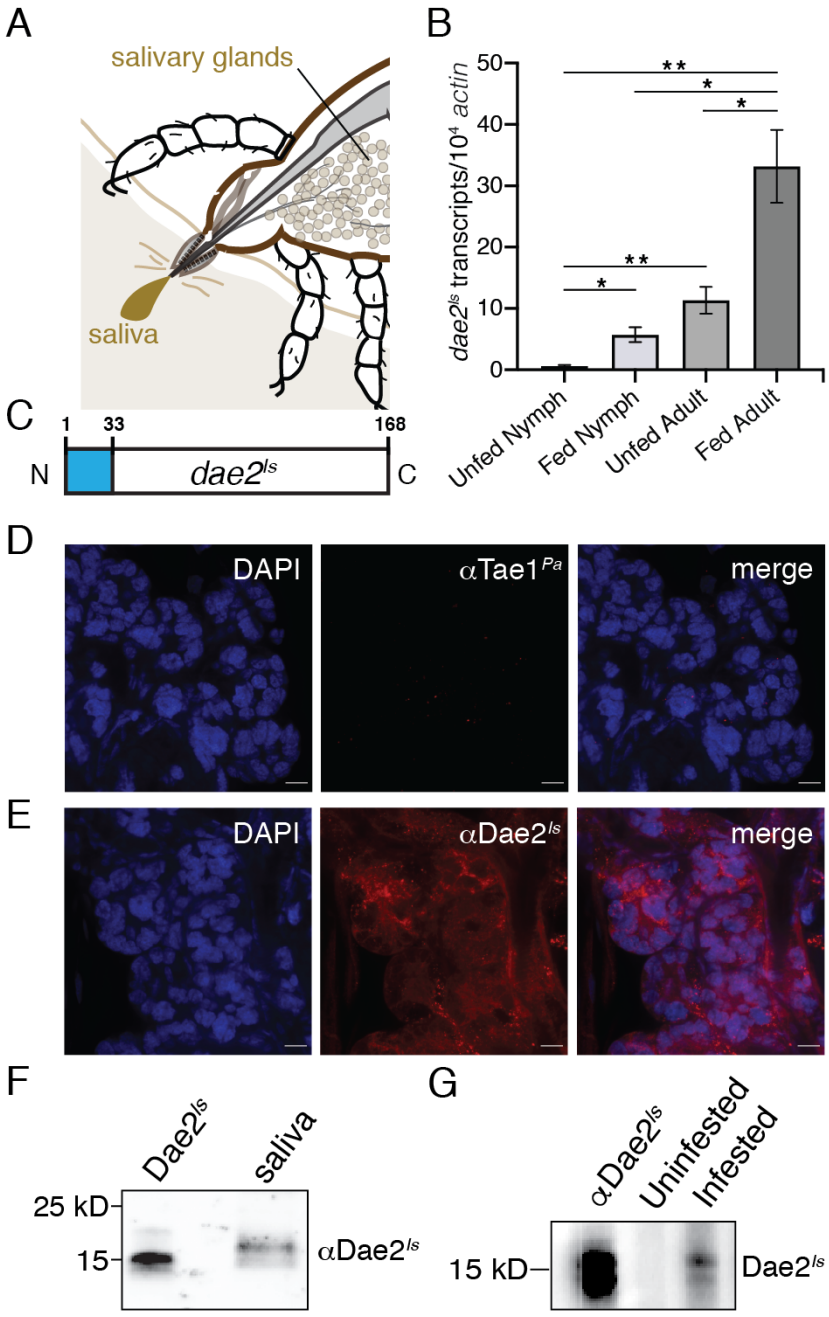

Figure 3: Regulation and localization of Dae2 in ticks during feeding. (**A**) Schematic of the tick at the bite-site interface showing the salivary glands. The salivary glands produce the saliva that is injected into the host. (**B**) *dae2*^{Is} expression (normalized against *actin*^{Is} transcripts) before (unfed) and after feeding (fed) on mice for nymph and adult ticks. * $p<0.05$, ** $p<0.01$ (**C**) Diagram of the *dae2*^{Is} gene structure showing the predicted N-terminal signal sequence from nucleotide position 1-33 (blue) (**D-E**) Confocal images of *I. scapularis* salivary glands from adult females. Whole mounts were immunostained with DAPI (left panels, blue), control rabbit antibody against Tae1^{Pa} (D middle, red) or rabbit αDae2^{Is} (E middle, red). Scale bars= 15µm. More examples shown in Figure S6 (**F**) Western blot of collected saliva from partially fed *I. scapularis* adult females demonstrating presence of Dae2^{Is} in saliva. First lane has recombinant Dae2^{Is} as a positive control for rabbit αDae2^{Is} reactivity. (**G**) Western blot showing reactivity of mouse serum to Dae2^{Is}. Recombinant Dae2 protein was probed with mouse serum before (Uninfested) or after *I. scapularis* feeding (Infested). Rabbit αDae2^{Is} was used as positive control for reactivity (first lane).

reason that *I. scapularis* ticks may have co-opted Dae2^{Is} to prevent contamination of host tissue and incoming bloodmeals during feeding. We therefore examined Dae2^{Is} regulation and localization during feeding. We quantified *dae2*^{Is} transcripts in ticks before and after a bloodmeal and found dramatic upregulation of *dae2*^{Is} expression in both nymph and adult ticks following consumption of a bloodmeal (Figure 3b). Dae2^{Is} has also previously been observed to increase in response to *B. burgdorferi*-infected bloodmeals[29]. Elevated levels of *dae2*^{Is} in feeding and infected ticks are indicative of an important functional role for Dae2^{Is} during this critical parasitic phase of the tick life cycle. The *dae2*^{Is} gene encodes a predicted N-terminal secretion signal (Figure 3c)[12], which suggests Dae2^{Is} could be secreted to the outside of tick salivary cells. Extracellular delivery of Dae2^{Is} into the bite site by way of tick saliva is a requisite for mediating tick–host–microbe interactions during feeding. Using immunofluorescence, we imaged Dae2^{Is} distribution in *I. scapularis* salivary glands by confocal microscopy and observed strong labeling of vesicle-like puncta in α-Dae2^{Is} but not control antibody conditions (Figure 3d-e, Figure S6). We also detected Dae2^{Is} in saliva harvested directly from partially-fed *I. scapularis* ticks (Figure 3f), suggesting Dae2^{Is} is secreted from vesicle-like structures into the extracellular milieu of excreted saliva. The slight variation in protein size of Dae2 from ticks and the recombinant protein from *E. coli* might arise from posttranslational modification in the tick. Importantly, blood sera collected from mice that had been fed on by *I. scapularis* ticks (infested) showed immunoreactivity to Dae2^{Is}, and this was not the case for uninfested mice that had never been exposed to ticks (Figure 3g), indicating that the tick injects Dae2^{Is} into the bite site where it is seen as an antigen for the murine immune system. From these results, we conclude that Dae2^{Is} is up-regulated during feeding and delivered to the bite site via saliva where it can physically access neighboring microbes, including bacteria that colonize host skin.

Importance of Dae2^{Is} for tick resistance to its own pathogens

Vertebrate host skin is colonized by microbial commensals that could infect the tick bite site during feeding, exposing ticks to a contaminated bloodmeal. It is possible host skin immunity prevents this from occurring. Alternatively, ticks themselves could employ salivary effectors, such as Dae2^{Is}, to protect against host skin microbes while feeding. We therefore asked whether disruption of Dae2^{Is} in *I. scapularis* nymphs affects levels of skin-associated bacteria in ticks during feeding. To test whether Dae2^{Is} activity affects acquisition or proliferation of these bacteria, we disrupted *dae2*^{Is} through microinjection-based RNA interference (RNAi) prior to feeding ticks on mice. In addition, we developed an approach to block pre-existing Dae2^{Is} protein stored in unfed tick salivary vesicles (Fig 3d-e and S6). Using an antibody generated against recombinant Dae2^{Is} (αDae2^{Is}), which we found blocks lytic activity of the enzyme *in vitro* (Figure S7), we pre-immunized mouse bloodmeal hosts, which would allow inhibition of Dae2^{Is} activity once delivered into the mice. Sterile saline was used as a control (Figure 4a). We retrieved ticks during the fast-feeding phase of their bloodmeals (day 3) and measured levels of skin-associated *Staphylococcus* in ticks by qPCR. Given the diversity of *Staphylococcus* commensal strains that colonize mouse skin, we used genus-specific primers to maximize the scope of our analysis (Supplementary Table 2). We found that ticks from the experimental *dae2*^{Is} group indeed supported higher levels of *Staphylococcus* bacteria than the control group (Figure 4b). We reasoned that bacteria, such as *S. epidermidis*[20,31], could negatively impact tick health when present at unusually high levels in the tick midgut. Thus, we investigated whether our *dae2*^{Is} ticks exhibited any feeding-related defects relative to the control group. We measured tick

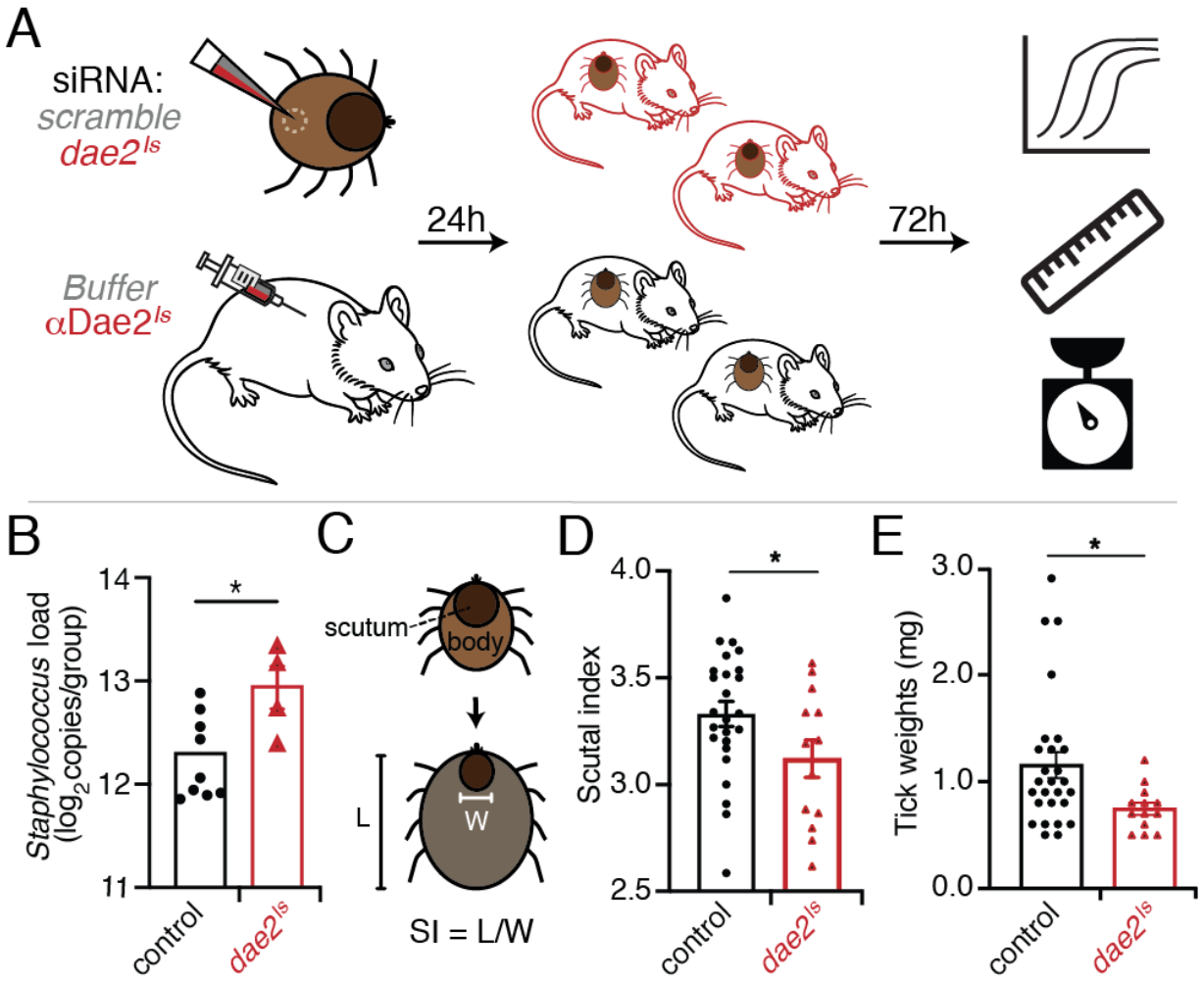

Figure 4: Dae2 activity affects tick fitness during feeding on mice. (A) Schematic of *in vivo* *dae2*^{Is} knockdown experiment. Mice were injected with sterile saline control (grey) or 2.5mg Rabbit αDae2^{Is} antibody and *I. scapularis* nymphs were microinjected with siRNAs targeting *dae2*^{Is} (red) or scrambled controls (grey). After 24 hour recovery, *dae2*^{Is} injected and scrambled injected ticks were placed on αDae2^{Is} antibody injected mice or control mice, respectively. Ticks were forcibly detached at 3 days and assessed by qPCR, scutal index, and weight. (**B**) *Staphylococcus* load was detected in DNA isolated from pooled *dae2*^{Is} knockdown (red) or control ticks (black) by qPCR with primers designed to target all species from the genus *Staphylococcus*. Results are presented as the average $\log_2$ *Staphylococcus* per tick. *$p<0.05$ with student's t-test. (**C**) Diagram of how scutal index (SI) changes during feeding. Scutal index is the ratio of the length of the entire tick body to the width of the scutum[30]. Scutal index (**D**) and tick weight (**E**) of individual ticks from experiment detailed in B. *$p<0.05$ based on student's t-test. Tick length and scutal width were measured from pictures with ImageJ. Weight was measured with an analytical balance with an error of +/- 0.1mg.

body expansion at day 3 by calculating scutal indices (SI), which typically report how long ticks have been feeding on a bloodmeal host (Figure 4c)[30]. We observed a notable difference in size between the two groups (Figure 4d). We also weighed individual ticks and found that *dae2*^{Is} ticks had significantly lower masses (Figure 4e), suggesting infection of ticks by host bacteria imposed a feeding-based fitness cost. This fitness cost may be due to slowed attachment, reduced feeding, or some combination of these, ultimately resulting in decreased blood intake or more prolonged, hazardous interactions with a bloodmeal host.

There are several mechanisms by which Dae2^{Is} could inhibit skin microbes, as observed in our *in vivo* feeding experiments. Dae2^{Is} could directly lyse bacteria present at the bite site or within the tick gut. Alternatively, Dae2^{Is} could function as a signaling module, akin to eukaryotic peptidoglycan recognition proteins (PGRPs), which activate or regulate downstream immunity cascades in response to PG recognition[32], or act through a combination of these mechanisms. In light of potent antibacterial activity we observe for Dae2^{Is} against skin microbes *in vitro*, we hypothesize that this enzyme directly kills *S. epidermidis* or other skin bacteria *in vivo*. To test this possibility, we assessed whether Dae2^{Is} can inhibit *S. epidermidis* in the tick by challenging ticks with *S. epidermidis*, coupled with biochemical inhibition of Dae2^{Is} activity. To inhibit this enzyme specifically within tick guts, we took advantage of the inhibitory αDae2^{Is} antibody used in our *in vivo* knockdown experiments (Figure S7). We needle-challenged tick midguts with *S. epidermidis* with or without αDae2^{Is} to quickly deplete Dae2^{Is} activity specifically within the tick midgut compartment and then asked whether this affects *S. epidermidis* levels in the tick (Figure 5a). Co-injection of αDae2^{Is} with *S. epidermidis* led to higher bacteria levels of *S. epidermidis* in ticks than bacteria alone at 4 hours post-injection, suggesting Dae2^{Is} has the capacity to directly antagonize *S. epidermidis in vivo* (Figure 5b) by killing or inhibiting the growth of cells. Interestingly, we also observed a concomitant increase in the death of the ticks themselves in the *Se*+αDae2^{Is} group (Figure 5c), not evident in the αDae2^{Is} control group. These effects demonstrate that there is a fitness cost to housing high levels of *S. epidermidis*, which is consistent with observations from our *in vivo* feeding experiments.

Together, these observations support a model in which bloodmeal host skin commensals are pathogenic to ticks, making Dae2^{Is}-dependent inhibition of *S. epidermidis* important for tick health. To our knowledge, our results identify the first known natural opportunistic pathogen of the tick disease vector *I. scapularis*. Future studies examining molecular and cellular changes at the host bite site will offer mechanistic insight into whether contamination of host tissues may also contribute to our observed phenotypes. Collectively, these data suggest that Dae2^{Is} provides the *I. scapularis* immune system with the ability to resist diverse bacteria, including bloodmeal host skin commensals that are frequently and intimately encountered by ticks. In contrast to stable tick-associated symbionts, such as *B. burgdorferi*, Staphylococcal bacteria that colonize host skin are infectious against *I. scapularis*, and tick resistance of these strains through Dae2^{Is} is important for the health and hematophagous lifestyle of ticks.

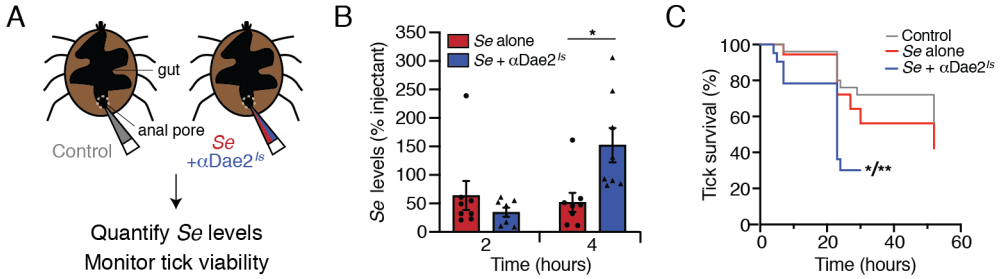

Figure 5: Dae2-dependent effects on *I. scapularis–S. epidermidis* interactions *in vivo*. (**A**) Schematic of experimental setup. *I. scapularis* nymphs were microinjected into the anal pore with a control antibody (grey, left), live *S. epidermidis* alone (red, right), or live *S. epidermidis* and αDae2^{Is} together (blue, right). Ticks were then monitored for levels of *S. epidermidis* and tick survival. (**B**) CFU levels of *S. epidermidis* alone (red) or together with αDae2^{Is} antibody to neutralize the lytic activity of Dae2^{Is} (blue) at 2 and 4 hours post injection. Results are shown as percentage of CFU at time 0 (injectant). *$p<0.05$ based on paired t-test. (**C**) Tick survival after microinjection of antibody control (grey), *S. epidermidis* alone (red), or *S. epidermidis* together with αDae2^{Is} antibody to neutralize the lytic activity of Dae2^{Is} (blue). *$p<0.05$ compared to *S. epidermidis* alone and **$p<0.01$ compared to antibody alone based on Log-rank (Mantel-Cox) test.

Discussion

Animals interact with diverse microbes, and whether a bacterium is beneficial or pathogenic is highly host-dependent [33]. Eukaryotes have evolved to respond appropriately; thus, the differential specificity of animal immune systems reflects how host–microbe interactions vary between organisms. Ticks harbor symbiotic microbes, such as *B. burgdorferi*, which are tolerated by their tick vector but are pathogenic to humans upon transmission[34]. In this study, we discovered that the opposite is also true: ticks are vulnerable to infection by bacterial commensals found on the skin of vertebrates they must feed on. Microbiota are important arms of animal physiology, and our observation that the domesticated tick immune factor Dae2 has evolved to target bacterial partners of vertebrate hosts highlights both the inseparability of these relationships and also the transmutable nature of microbial interactions across different biological contexts. Animals not only clash with each other but also with associated microbes, which are an integral part of an organismal "package." Particularly for blood-feeding parasites, such as ticks, successful navigation of these complex, interkingdom clashes is critical for survival.

This study revealed mechanisms by which the tick vector *I. scapularis* has evolved to mediate such a clash. The phylogenetic history of *dae2* as a horizontally transferred gene from bacteria granted us the unique opportunity to investigate how this immune effector has structurally, biochemically, and functionally diverged from its ancestral form to support the unique biology of ticks[12]. Invertebrates rely solely on innate immunity to distinguish between virulent and benign bacteria by employing pattern recognition receptors (PRRs) that recognize conserved microbe-associate molecular patterns (MAMPs), phagocytic cells, and a variety of humoral downstream effectors, including antimicrobial peptides (AMPs) and lytic enzymes[35-37]. These defense mechanisms can vary in their location, timing, and sensitivity to microbial signatures, contributing to the overall specificity of invertebrate–microbe interactions[38,39]. We discovered that Dae2^{Is} has evolved the capacity to selectively kill skin-associated bacteria of their bloodmeal hosts, and that these microbes pose a threat to tick health. The timing and location of Dae2^{Is} action in the saliva of ticks further contributes to its specific role in protecting against host microbes during feeding, suggesting this function is of biological importance to ticks.

Ticks have a very different relationship with its own symbiont *B. burgdorferi*, which stably colonizes the tick midgut and is maintained through a multi-host zoonotic lifecycle[4]. Although Dae2^{Is} does have the capacity to degrade purified *B. burgdorferi* PG, we did not detect direct killing of intact *B. burgdorferi.* We did, however, previously observe a modest but significant increase in *B. burgdorferi* levels in *dae2*^{Is} knockdown ticks[12]. The *I. scapularis* genome encodes functional homologs for several canonical innate immune signaling pathways [34,40], which can be activated through PG fragments. Thus, *dae2*-dependent inhibition of *B. burgdorferi* may have resulted from altered immune signaling in response to *B. burgdorferi* PG processing by Dae2^{Is}. Alternatively, Dae2^{Is} may act in synergy with an additional host factor, such as membrane-permeabilizing antimicrobial peptides. Although limited, the ability of this effector to control a known symbiont may suggest that *I. scapularis* tolerance of *B. burgdorferi* is dependent on the ability of the tick to restrict *B. burgdorferi* proliferation to levels that are not detrimental to its own health.

More broadly, expansion of antimicrobial strategies was likely a key facilitator for the parasitic lifestyle of hematophagous arthropods. The rise of blood-feeding behavior over the

course of arthropod evolution was concomitant with the emergence of numerous antibacterial genes, such as *dae2*, that are expressed in saliva[41]. The intriguing timing of *dae2* acquisition by ticks and mites soon after the emergence of hematophagy within this arthropod clade[12] might indicate that Dae2 activity was an important enabler of blood-feeding. Hard ticks imbibe blood continuously from one host for several days at a time, leading to exceptionally intimate and sustained interactions with a wide range of vertebrates and associated microbes[42]. Our observations suggest that $dae2^{Is}$ ensures successful *I. scapularis* feeding by protecting ticks against infectious bacteria near host attachment sites. Antimicrobial activity in tick saliva could also provide a secondary benefit of blocking contamination of the bite site itself, preventing a cascade of antagonistic host responses. Hundreds of other tick salivary proteins await functional characterization[28,43,44] and will likely unveil novel aspects of relationships between hosts and this important class of disease vectors.

References

(1) Mans, B. J.; Neitz, A. W. H. *Insect Biochemistry and Molecular Biology* **2004**, *34* (1), 1–17.

(2) Mans, B. J. *JIN* **2011**, *3* (1), 41–51.

(3) Ribeiro, J. M.; Makoul, G. T.; Levine, J.; Robinson, D. R.; Spielman, A. *Journal of Experimental Medicine* **1985**, *161* (2), 332–344.

(4) Sonenshine, D. E. In *Tick-Borne Diseases of Humans*; American Society of Microbiology, 2005; pp 12–36.

(5) Ribeiro, J. M. C.; Francischetti, I. M. B. *Annu. Rev. Entomol.* **2003**, *48* (1), 73–88.

(6) Nuttall, P. A. *Wien. Klin. Wochenschr.* **2019**, *2528* (1), 1–12.

(7) Gillespie, R. D.; Mbow, M. L.; Titus, R. G. *Parasite Immunol.* **2000**, *22* (7), 319–331.

(8) Narasimhan, S.; Booth, C. J.; Deponte, K.; Wu, M.-J.; Liang, X.; Mohanty, S.; Kantor, F.; Fikrig, E. *Ticks Tick Borne Dis* **2019**, *10* (2), 386–397.

(9) Smith, A. A.; Pal, U. *Front Cell Infect Microbiol* **2014**, *4* (26), 116.

(10) Hajdušek, O.; Síma, R.; Ayllón, N.; Jalovecká, M.; Perner, J.; la Fuente, de, J.; Kopáček, P. *Front Cell Infect Microbiol* **2013**, *3*, 26.

(11) Kopáček, P. In *Encyclopedia of Parasitology*; Springer Berlin Heidelberg: Berlin, Heidelberg, 2015; pp 1–4.

(12) Chou, S.; Daugherty, M. D.; Peterson, S. B.; Biboy, J.; Yang, Y.; Jutras, B. L.; Fritz-Laylin, L. K.; Ferrin, M. A.; Harding, B. N.; Jacobs-Wagner, C.; Yang, X. F.; Vollmer, W.; Malik, H. S.; Mougous, J. D. *Nature* **2015**, *518* (7537), 98–101.

(13) Russell, A. B.; Hood, R. D.; Bui, N. K.; LeRoux, M.; Vollmer, W.; Mougous, J. D. *Nature* **2011**, *475* (7356), 343–347.

(14) Russell, A. B.; Singh, P.; Brittnacher, M.; Bui, N. K.; Hood, R. D.; Carl, M. A.; Agnello, D. M.; Schwarz, S.; Goodlett, D. R.; Vollmer, W.; Mougous, J. D. *Cell Host Microbe* **2012**, *11* (5), 538–549.

(15) Husnik, F.; McCutcheon, J. P. *Nature Reviews Microbiology* **2018**, *16* (2), 67–79.

(16) Tokarz, R.; Tagliafierro, T.; Sameroff, S.; Cucura, D. M.; Oleynik, A.; Che, X.; Jain, K.; Lipkin, W. I. *Ticks Tick Borne Dis* **2019**, *10* (4), 894–900.

(17) Díaz-Sánchez, S.; Hernández-Jarguín, A.; Torina, A.; de Mera, I. G. F.; Blanda, V.; Caracappa, S.; Gortazar, C.; la Fuente, de, J. *Ticks Tick Borne Dis* **2019**, *10* (2), 336–343.

(18) Ross, B. D.; Hayes, B.; Radey, M. C.; Lee, X.; Josek, T.; Bjork, J.; Neitzel, D.; Paskewitz, S.; Chou, S.; Mougous, J. D. *ISME J* **2018**, *12* (11), 2596–2607.

(19) Hernández-Jarguín, A.; Díaz-Sánchez, S.; Villar, M.; la Fuente, de, J. *Ticks Tick Borne Dis* **2018**, *9* (5), 1241–1251.

(20) Greay, T. L.; Gofton, A. W.; Paparini, A.; Ryan, U. M.; Oskam, C. L.; Irwin, P. J. *Parasit Vectors* **2018**, *11* (1), 12–14.

(21) Narasimhan, S.; Schuijt, T. J.; Abraham, N. M.; Rajeevan, N.; Coumou, J.; Graham, M.; Robson, A.; Wu, M.-J.; Daffre, S.; Hovius, J. W.; Fikrig, E. *Nat Commun* **2017**, *8* (1), 184–17.

(22) Sanz-Gaitero, M.; Keary, R.; Garcia-Doval, C.; Coffey, A.; van Raaij, M. J. *Virol. J.* **2014**, *11* (1), 133.

(23) Turner, R. D.; Vollmer, W.; Foster, S. J. *Molecular Microbiology* **2014**, *91* (5), 862–874.
(24) Narasimhan, S.; Fikrig, E. *Trends Parasitol.* **2015**, *31* (7), 315–323.
(25) Jutras, B. L.; Scott, M.; Parry, B.; Biboy, J.; Gray, J.; Vollmer, W.; Jacobs-Wagner, C. *Proc. Natl. Acad. Sci. U.S.A.* **2016**, *113* (33), 9162–9170.
(26) Jutras, B. L.; Lochhead, R. B.; Kloos, Z. A.; Biboy, J.; Strle, K.; Booth, C. J.; Govers, S. K.; Gray, J.; Schumann, P.; Vollmer, W.; Bockenstedt, L. K.; Steere, A. C.; Jacobs-Wagner, C. *Proc. Natl. Acad. Sci. U.S.A.* **2019**, *116* (27), 13498–13507.
(27) Bernard, K. *Journal of Clinical Microbiology* **2012**, *50* (10), 3152–3158.
(28) Kim, T. K.; Tirloni, L.; Pinto, A. F. M.; Moresco, J.; Yates, J. R.; da Silva Vaz, I.; Mulenga, A. *PLOS Negl Trop Dis* **2016**, *10* (1), e0004323.
(29) Smith, A. A.; Navasa, N.; Yang, X.; Wilder, C. N.; Buyuktanir, O.; Marques, A.; Anguita, J.; Pal, U. *Cell Host Microbe* **2016**, *20* (1), 91–98.
(30) Meiners, T.; Hammer, B.; Göbel, U. B.; Kahl, O. *Int. J. Med. Microbiol.* **2006**, *296 Suppl 40*, 103–107.
(31) Narasimhan, S.; Fikrig, E. *Trends Parasitol.* **2015**, *31* (7), 315–323.
(32) Dziarski, R.; Gupta, D. *Genome Biol.* **2006**, *7* (8), 232.
(33) Ehrlich, G. D.; Hiller, N. L.; Hu, F. Z. *Genome Biol.* **2008**, *9* (6), 225–227.
(34) Shaw, D. K.; Tate, A. T.; Schneider, D. S.; Levashina, E. A.; Kagan, J. C.; Pal, U.; Fikrig, E.; Pedra, J. H. F. *Trends Immunol.* **2018**, *39* (11), 862–873.
(35) Little, T. J.; Hultmark, D.; Read, A. F. *Nature Immunology* **2005**, *6* (7), 651–654.
(36) Schulenburg, H.; Boehnisch, C.; Michiels, N. K. *Mol. Immunol.* **2007**, *44* (13), 3338–3344.
(37) Humphreys, T.; Reinherz, E. L. *Immunology Today* **1994**, *15* (7), 316–320.
(38) Bosch, T. C. G.; Guillemin, K.; McFall-Ngai, M. *Bioessays* **2019**, *41* (10), e1800256.
(39) McFall-Ngai, M.; Hadfield, M. G.; Bosch, T. C. G.; Carey, H. V.; Domazet-Lošo, T.; Douglas, A. E.; Dubilier, N.; Eberl, G.; Fukami, T.; Gilbert, S. F.; Hentschel, U.; King, N.; Kjelleberg, S.; Knoll, A. H.; Kremer, N.; Mazmanian, S. K.; Metcalf, J. L.; Nealson, K.; Pierce, N. E.; Rawls, J. F.; Reid, A.; Ruby, E. G.; Rumpho, M.; Sanders, J. G.; Tautz, D.; Wernegreen, J. J. *Proc. Natl. Acad. Sci. U.S.A.* **2013**, *110* (9), 3229–3236.
(40) Gulia-Nuss, M.; Nuss, A. B.; Meyer, J. M.; Sonenshine, D. E.; Roe, R. M.; Waterhouse, R. M.; Sattelle, D. B.; la Fuente, de, J.; Ribeiro, J. M.; Megy, K.; Thimmapuram, J.; Miller, J. R.; Walenz, B. P.; Koren, S.; Hostetler, J. B.; Thiagarajan, M.; Joardar, V. S.; Hannick, L. I.; Bidwell, S.; Hammond, M. P.; Young, S.; Zeng, Q.; Abrudan, J. L.; Almeida, F. C.; Ayllón, N.; Bhide, K.; Bissinger, B. W.; Bonzon-Kulichenko, E.; Buckingham, S. D.; Caffrey, D. R.; Caimano, M. J.; Croset, V.; Driscoll, T.; Gilbert, D.; Gillespie, J. J.; Giraldo-Calderón, G. I.; Grabowski, J. M.; Jiang, D.; Khalil, S. M. S.; Kim, D.; Kocan, K. M.; Koči, J.; Kuhn, R. J.; Kurtti, T. J.; Lees, K.; Lang, E. G.; Kennedy, R. C.; Kwon, H.; Perera, R.; Qi, Y.; Radolf, J. D.; Sakamoto, J. M.; Sánchez-Gracia, A.; Severo, M. S.; Silverman, N.; Šimo, L.; Tojo, M.; Tornador, C.; Van Zee, J. P.; Vázquez, J.; Vieira, F. G.; Villar, M.; Wespiser, A. R.; Yang, Y.; Zhu, J.; Arensburger, P.; Pietrantonio, P. V.; Barker, S. C.; Shao, R.; Zdobnov, E. M.; Hauser, F.; Grimmelikhuijzen, C. J. P.; Park, Y.; Rozas, J.; Benton, R.; Pedra, J. H. F.; Nelson, D. R.; Unger, M. F.; Tubio, J. M. C.; Tu, Z.; Robertson, H. M.; Shumway, M.;

Sutton, G.; Wortman, J. R.; Lawson, D.; Wikel, S. K.; Nene, V. M.; Fraser, C. M.; Collins, F. H.; Birren, B.; Nelson, K. E.; Caler, E.; Hill, C. A. *Nat Commun* **2016**, *7*, 10507.

(41) disease, J. R. I. A. A.; 1995. *europepmc.org*

.

(42) Sonenshine, D. E. *Biology of ticks. Vol. I*; 1991.

(43) Chmelař, J.; Kotál, J.; Karim, S.; Kopáček, P.; Francischetti, I. M. B.; Pedra, J. H. F.; Kotsyfakis, M. *Trends Parasitol.* **2016**, *32* (3), 242–254.

(44) Perner, J.; Kropáčková, S.; Kopáček, P.; Ribeiro, J. M. C. *PLOS Negl Trop Dis* **2018**, *12* (4), e0006410.

(45) Van Duyne, G. D.; Standaert, R. F.; Karplus, P. A.; Schreiber, S. L.; Clardy, J. *J. Mol. Biol.* **1993**, *229* (1), 105–124.

(46) MacDowell, A. A.; Celestre, R. S.; Howells, M.; McKinney, W.; Krupnick, J.; Cambie, D.; Domning, E. E.; Duarte, R. M.; Kelez, N.; Plate, D. W.; Cork, C. W.; Earnest, T. N.; Dickert, J.; Meigs, G.; Ralston, C.; Holton, J. M.; Alber, T.; Berger, J. M.; Agard, D. A.; Padmore, H. A. *J Synchrotron Radiat* **2004**, *11* (Pt 6), 447–455.

(47) Liebschner, D.; Afonine, P. V.; Baker, M. L.; Bunkoczi, G.; Chen, V. B.; Croll, T. I.; Hintze, B.; Hung, L. W.; Jain, S.; Mccoy, A. J.; Moriarty, N. W.; Oeffner, R. D.; Poon, B. K.; Prisant, M. G.; Read, R. J.; Richardson, J. S.; Richardson, D. C.; Sammito, M. D.; Sobolev, O. V.; Stockwell, D. H.; Terwilliger, T. C.; Urzhumtsev, A. G.; Videau, L. L.; Williams, C. J.; Adams, P. D. *Acta Crystallogr D Struct Biol* **2019**, *75* (10), 861–877.

(48) Emsley, P. **2017**.

(49) Holm, L.; Rosenström, P. *Nucleic Acids Res.* **2010**, *38* (Web Server issue), W545–W549.

(50) Pettersen, E. F.; Goddard, T. D.; Huang, C. C.; Couch, G. S.; Greenblatt, D. M.; Meng, E. C.; Ferrin, T. E. *J Comput Chem* **2004**, *25* (13), 1605–1612.

(51) Kelley, L. A.; Mezulis, S.; Yates, C. M.; Wass, M. N.; Sternberg, M. J. E. *Nat Protoc* **2015**, *10* (6), 845–858.

(52) Glauner, B. *Anal. Biochem.* **1988**, *172* (2), 451–464.

(53) Kolesnikova, T. D.; Semeshin, V. F.; Andreyeva, E. N.; Zykov, I. A.; Kokoza, E. B.; Kalashnikova, D. A.; Belyaeva, E. S.; Zhimulev, I. F. *Fly (Austin)* **2011**, *5* (3), 181–190.

(54) Rego, R. O. M.; Bestor, A.; Rosa, P. A. *J. Bacteriol.* **2011**, *193* (5), 1161–1171.

Acknowledgments: We are grateful to George Meigs and James Holton at the Advance Light Source (Lawrence Berkeley National Laboratory), the Stroud lab (UCSF) and Michael Thompson (Fraser lab, UCSF) for help with X-ray crystallography. We thank Carol Gross, Tiffany Scharschmidt and Joe Bondy-Denomy (all at UCSF) as well as Patricia Rosa (Rocky Mountain Laboratories, NIAID, NIH) for providing bacterial strains. We also appreciate Dyche Mullins and Samuel Lord (UCSF) for their assistance with microscopy. The Chou lab thanks Soraya Pedemonte and Ethel Enoex-Godonoo for lab and administrative help, respectively, without which the lab would not run as smoothly. We are also grateful to Harmit Malik (UCSF), Carol Gross (UCSF), Wallace Marshall (UCSF), Tiffany Scharschmidt (UCSF), and the entire Chou lab for helpful discussions and review of the manuscript.

Funding: This project was funded in part by NIH grants (R01AI132851 to SC, R01AI134696 to JP), Research Councils UK (EP/T002778/1) to WV, and UCSF Program for Breakthrough Biomedical Research, funded in part by the Sandler Foundation (to SC). Additional support for SC came from the Chan Zuckerberg Biohub the Johnson & Johnson WiSTEM2D Award. FY was supported by the National Science Foundation (1650113) and a grant to UCSF from the Howard Hughes Medical Institute through the James H. Gilliam Fellowships for Advanced Study program.

Author contributions: Conceptualization SC, BH, AR; Formal analysis KL; Funding acquisition SC, FY, JHFP, WV; Investigation BH, AR, FY, SF, JK, LM, JB, ZZ, VB; Methodology BH, AR, KL, WV, JHFP, SC; Project administration SC; Resources WV, KL, JHFP; Software KL; Supervision SC, WV, JHFP; Visualization SC, BH, AR, KL, ZZ; Writing (original draft) SC, BH, AR; Writing (review & editing) SC, BH, AR, JHFP, WV

Competing interests: Authors declare no competing interests.

Data and materials availability: Tae2St crystal structure data is available in the RCSB PDB database (PDB ID: 6W1N)